ISSN 0915-633X

NATIONAL INSTITUTE FOR FUSION SCIENCE

Theoretical Study of Structure of Electric Field in Helical Toroidal Plasmas

S. Toda and K. Itoh

(Received - June 14, 2001)

NIFS-704 June 2001

RESEARCH REPORT
NIFS Series

TOKI, JAPAN

Theoretical study of structure of electric field in helical toroidal plasmas

S. TODA AND K. ITOH

National Institute for Fusion Science, Oroshi-cho 322-6, Toki, 509-5292, Japan

A set of transport equations is analyzed, including the bifurcation of the electric field. The structure of the electric field is studied by use of the theoretical model for the anomalous transport diffusivities. The steep gradient of the electric field is obtained at the electric domain. The suppression of the anomalous transport diffusivity is studied in the presence of the strong shear of the electric field The hard transition with the multiple ambipolar solutions is examined in the structure of the radial electric field. The details of the structure of the electric domain interface are investigated.

Key words helical plasmas, radial electric field, transport barrier, electric domain

1 Introduction

Many types of the improved confinement states have been found in toroidal plasmas. Among the variety of the improved confinement states, the H-mode in tokamaks has been studied most intensively. Through evolution of research, it is widely recognized that the structure of the electric field influences the various improved confinement modes. Nevertheless, quantitative analysis of the generation and the structure of the radial electric field in the high temperature plasmas is far from satisfactory. Study of the confinement mechanisms has also been done for helical plasmas [1].

Recently, the internal transport barrier has been found in electron cyclotron resonance heating (ECRH) plasma in the compact helical system (CHS) and the steep gradient in the profile of the radial electric field has been obtained in the inner region [2]. In Wendelstein7-AS (W7-AS), studies on the change of the electron transport triggered by the neoclassical transport have also been done theoretically [3] and experimentally [4, 5]. More recently, a change in the anomalous transport in the central region has also been reported in W7-AS. To study the existence of the transport barrier in the experimental conditions of helical plasmas, an investigation of the electric field bifurcation is needed. The interface of domains with different electric polarities has been pointed out for helical plasmas. It is well known that neoclassical transport dominant in the bipolar part of the particle flux in helical plasmas and multiple solutions of the ambipolar condition are allowed [6]. To study the interface of neighboring domains with different electric polarities, one-dimensional transport analysis is needed. We have examined the one-dimensional transport equations which describe the temporal evolutions of the density, the electron and ion temperatures, and the radial electric field in a cylindrical heliotron configuration in order to examine the detailed structure of

electric domain [7]. There are two important issues. The first is the formation of the electric field domain, which is associated with the steep gradient of E_r. The generation of the electric field in helical systems could be investigated more quantitatively because the neoclassical transport is found to play the dominant role in generating the radial electric field [6, 8]. The second is the study of the turbulent transport and the neoclassical energy transport so as to understand the formation of the internal transport barrier.

In order to analyze the structure of the electric field quantitatively, the self-consistent transport study is done in which both the electric field bifurcation and suppression of the anomalous transport are included. Here, we use the transport model (e.g. [1]) for anomalous diffusivities to describe the turbulent plasma. The reduction of the anomalous transport diffusivities is obtained due to the strong electric field shear at the electric domain. The hard transition of E_r which induces the steep gradient is examined. The neoclassical diffusivities are found to have a peak near the domain interface where the electric field vanishes. In this article, the structure of the electric domain interface is examined in detail.

2 One-dimensional model transport equations

In this section, the model equations used here are shown. The cylindrical coordinate is used and r-axis is taken in the radial cylindrical plasma in this article. The region $0 \leq r \leq a$ is considered, where a is the minor radius. The expression for the radial neoclassical flux associated with helical-rippled trapped particle is given as [9]

$$\Gamma_j^{na} = -\epsilon_t^2 \sqrt{\epsilon_h} v_{dj}^2 n_j \int_0^\infty dx x^{\frac{5}{2}} e^{-x} \widetilde{\nu}_j \frac{A_j(x, E_r)}{\omega_j^2(x, E_r)}, \tag{1}$$

where $x \equiv m_j v^2/(2T_j)$, $A_j(x, E_r) = n_j'/n_j - Z_j e E_r/T_j + (x-3/2)T_j'/T_j$, $\omega_j^2(x, E_r) = 3\widetilde{\nu}_j^2(x) + 1.67(\epsilon_t/\epsilon_h)(\omega_E + \omega_{Bj})^2 + (\epsilon_t/\epsilon_h)^{\frac{3}{2}}\omega_{Bj}^2/4 + 0.6\,|\omega_{Bj}|\,\widetilde{\nu}_j$ and $\widetilde{\nu}_j(x) = \nu_{thj}/(\epsilon_h x^{\frac{3}{2}})$. Here, the relations $\omega_E = -E_r/(rB)$, $\omega_{Bj} = -T_j \epsilon_h' x/(Z_j e r B)$ and $v_{dj} = -T_j/(Z_j e r B)$ are used. The quantities m_j, n_j, T_j, ν_{thj} are the mass, the density, the temperature, the collision frequency using the thermal velocity for the species j and the parameters ϵ_t and ϵ_h are the toroidal and helical ripple, respectively. The prime denotes the derivative with respect to the radial direction. This expression for the particle flux is the connection formula and is applicable to both the collisionless and collisional regimes. The total particle flux Γ^t is written as

$$\Gamma^t = \Gamma^{na} - D_a \frac{\partial n}{\partial r}. \tag{2}$$

Here, D_a is the anomalous particle diffusivity. The energy flux related with neoclassical ripple transport is given as [9]

$$Q_j^{na} = q_j^{na} + \frac{5}{2}\Gamma_j^{na} T_j = -\epsilon_t^2 \sqrt{\epsilon_h} v_{dj}^2 n_j T_j \int_0^\infty dx x^{\frac{7}{2}} e^{-x} \widetilde{\nu}_j(x) \frac{A_j(x, E_r)}{\omega_j^2(x, E_r)}. \tag{3}$$

The total heat flux Q_j^t of the species j is written as

$$Q_j^t = Q_j^{na} - n\chi_a \frac{\partial T_j}{\partial r}. \tag{4}$$

Here, χ_a is the anomalous heat diffusivity. The theoretical model for the anomalous heat conductivity obtained by the eigenvalue problem for the ballooning mode and the interchange mode is adopted and will be explained later. The neoclassical diffusion coefficient for the electric field is expressed by [10]

$$D_{E_j} = -\frac{e}{\epsilon_\perp}\frac{3}{16\sqrt{2\pi}}\frac{Z_j e}{T_j}\frac{n_j \nu_{thj} T_j^4}{(Z_j e)^4}\frac{\epsilon_t^4}{\sqrt{\epsilon_h}}\left(1+\frac{\epsilon_t}{\epsilon_h}\right)\int_{x_b}^{\infty}\frac{dx e^{-x}x^3}{\left(|E_r| + \left|x\frac{T_j}{Z_j e}\epsilon_h'\right|\right)^4}, \tag{5}$$

where $x_b = [\nu_{thj}/(\epsilon_h(|E_r| + |T_j/(Z_j e)\epsilon_h'|))]^{2/3}$. The anomalous diffusion coefficient for the radial electric field is denoted by D_{Ea}.

The equation for the density is

$$\frac{\partial n}{\partial t} = -\frac{1}{r}\frac{\partial}{\partial r}(r\Gamma^t) + S_n, \tag{6}$$

the term S_n represents the particle source such as the ionization effect. The equation for the electron temperature is given as

$$\frac{3}{2}\frac{\partial}{\partial t}(nT_e) = -\frac{1}{r}\frac{\partial}{\partial r}(rQ_e^t) - \frac{m_e}{m_i}\frac{n}{\tau_e}(T_e - T_i) + P_{he}, \tag{7}$$

where the term τ_e denotes the electron collision time and the second term in the right hand side represents the heat exchange between ions and electrons. The term P_{he} represents the absorbed power due to the ECRH heating and its profile is assumed to be proportional to $\exp(-(r/(0.2a))^2)$ for simplicity. The equation for the ion temperature is

$$\frac{3}{2}\frac{\partial}{\partial t}(nT_i) = -\frac{1}{r}\frac{\partial}{\partial r}(rQ_i^t) + \frac{m_e}{m_i}\frac{n}{\tau_e}(T_e - T_i) + P_{hi}. \tag{8}$$

The term P_{hi} represents the absorbed power of ions and its profile is also assumed to be proportional to $\exp(-(r/(0.2a))^2)$.

The radial electric field equation in a nonaxisymmetric system is expressed by [10]

$$\frac{\partial E_r}{\partial t} = -\frac{e}{\epsilon_\perp}\sum_j Z_j \Gamma_j^{na} + \frac{1}{r}\frac{\partial}{\partial r}\left(\sum_j Z_j (D_{Ej} + D_{Ea}) r \frac{\partial E_r}{\partial r}\right), \tag{9}$$

where $\epsilon_\perp$ is the perpendicular dielectric coefficient as $\epsilon_\perp = \epsilon_0((c^2/v_A^2)+1)(1+2q^2)$. Here, ϵ_0 is the dielectric constant in the vacuum, c is the speed of light, v_A is the velocity of Alfvén wave and q is the safety factor. The parameter Z_j is a charge number of the species j. The factor $(1+2q^2)$ is introduced from the toroidal effect. Equation (9) is solved together with the density and the temperature (ion and electron) equations (6), (7) and (8).

3 Boundary conditions and the model of anomalous transport coefficients

The density, temperature and electric field equations (6)-(9) are solved under the appropriate boundary conditions. We fix the boundary condition at the center of the plasma (r=0) such that $n' = T_e' = T_i' = E_r(= -\phi') = 0$, where ϕ is the electrostatic potential of the electric field. For the diffusion equation of the radial electric field, the boundary condition at the edge (r=a) is chosen as $\sum_j Z_j \Gamma_j = 0$. This simplification is employed because the electric field bifurcation in the core plasma is the main subject of this study. The boundary conditions at the edge (r=a) with respect to the density are those expected CHS device: $-n/n' = 0.05(m)$, $-T_e/T_e' = -T_i/T_i' = 0.02(m)$.

The machine parameters are similar to those of CHS device, such as $R = 1(m)$, $a = 0.2(m)$, the toroidal magnetic field $B = 1(T)$, toroidal mode number $m = 8$ and the poloidal mode number $\ell = 2$. We set the safety factor and the helical ripple coefficient as $q = 3.3 - 3.8(r/a)^2 + 1.5(r/a)^4$ and $\varepsilon_h = 0.231(r/a)^2 + 0.00231(r/a)^4$, respectively [2]. The particle source S_n is set to be $S_n = S_0 \exp((r-a)/L_0)$, where L_0 is set to be $0.01(m)$ and the value of S_0 is strongly influenced by the particle confinement time.

The value for the anomalous diffusivities of the particle and the electric field is chosen $D_a = 10(m^2 s^{-1})$. This value is set to be constant spatially and temporally. In this study, we adopt the model for the anomalous heat conductivity based on the theory of the self-sustained turbulence due to the ballooning mode and the interchange mode, both driven by the current diffusivity. The reduction of the anomalous transport due to the inhomogeneous radial electric field was reported in the toroidal helical system. The anomalous transport coefficient for the temperatures is given as $\chi_a = \chi_0/(1+G\omega_{E1}^2)$, where $\chi_0 = F(s,\alpha)\alpha^{\frac{3}{2}} c^2 v_A/(\omega_{pe}^2 qR)$, where ω_{pe} is the electron plasma frequency. The factor $F(s,\alpha)$ is the function of the magnetic shear s and the normalized pressure gradient α, defined by $s = rq'/q$ and $\alpha = -q^2 R\beta'$. For the ballooning mode turbulence for the system with a magnetic well, we employ the anomalous thermal conductivity $\chi_{a,BM}$ [11]: $F_{BM} = C/\sqrt{2(1-2s_1)(1-2s_1+3s_1^2)}$ $(s_1 < 0)$ and $F_{BM} = C(1+9\sqrt{2}{s_1}^{5/2})/(\sqrt{2}(1-2s_1+3{s_1}^2+2{s_1}^3)$ $(s_1 > 0)$, where $s_1 = s-\alpha$ for the negative pressure gradient and $s_1 = \alpha - s$ for the positive pressure gradient. The factor for the suppression due to the electric field shear $\omega_{E1} = a\tau_{AP}E_r'/(s\tau B)$, $G = 1/(2\alpha^2)$, where $\tau_{AP} = a\sqrt{\mu_0 m_i \bar{n}}/B_p$. In the case of the interchange mode turbulence [1], the factor F has been given by $F_{IM} = 3C(\Omega'/2)^{\frac{3}{2}}(R/a)^{\frac{3}{2}}/(qs^2)$, where $\Omega' = (r/R)^2(m/\ell)(r/a)^{-2}((r/a)^4/q)'$ for the anomalous heat conductivity $\chi_{a,IM}$. The factor for the suppression due to the electric field shear is $\omega_{E1} = \tau_{AP}E_r'/B$ and $G = 0.52D_0^{-1}$, where $D_0 = \Omega'\beta' a^2 R^2/(2\tau^2)$. For the standard parameters in CHS experiment, the numerical factor C is chosen to be 10. We use this value of C throughout this paper. The greater one of the two diffusivities is adopted, $\chi_a = \max(\chi_{a,BM}, \chi_{a,IM})$. The approximation $D_{Ea} = \chi_a$ is employed, where the validity of this approximation is discussed in ref. [12].

In order to set the averaged temperature of electrons to be around $250(eV)$ and the density to be around $1 \times 10^{19}(m^{-3})$, the absorbed power of electrons is $100(kW)$ and the coefficient S_0 is $7 \times 10^{24}(m^{-3}s^{-1})$ for the choice of above values of the anomalous transport coefficients. The averaged ion temperature $\bar{T}_i$ is chosen to be about $T_i = 150(eV)$, where the absorbed power of ions is fixed at $50kW$.

4 Results of analysis

Using the parameters and boundary conditions given, we analysis equations (1)-(4). The stationary solutions of the radial electric field are shown in figure 1(a) for $\bar{n} = 1 \times 10^{19}$, $\bar{T}_e = 250(eV)$ and $\bar{T}_i = 150(eV)$. The density and the temperature profiles of the electrons and the ions are shown in figures 1(b) and (c), respectively. In figure 1(c), the dashed curve represents the case of the ion temperature and the full curve shows the profile of the electron temperature, respectively. At the point $(r = r_T(0.12m))$, the transition of the radial electric field is found. The circles in figure 1(a) show the values of the electric field which satisfy the local ambipolar condition for the calculated profiles of the density and the temperatures of figure 1(b) and (c). Multiple solutions are allowed for the local ambipolar condition in the parameter region examined here. We call the hard transition when multiple

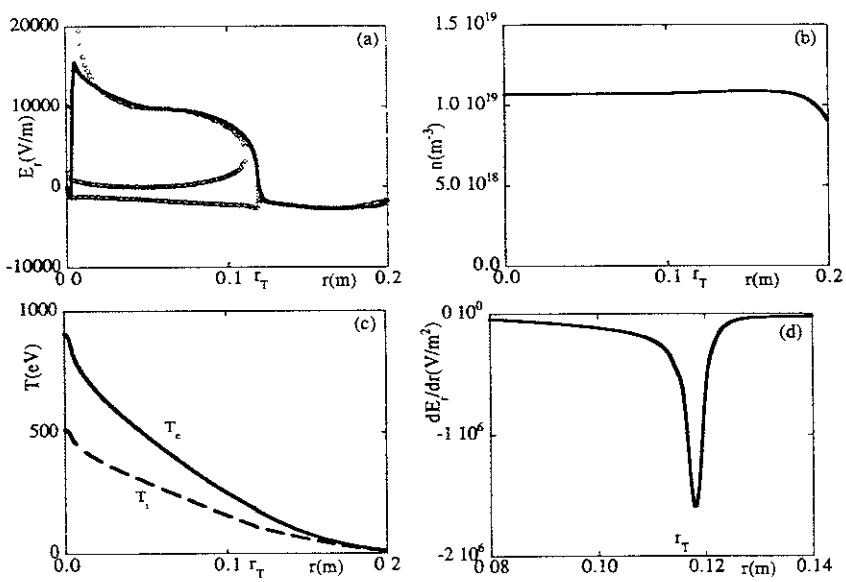

Fig. 1. (a) Radial dependence of the electric field (full curve); circles show the electric field derived from the ambipolar condition. (b) Radial profile of the density and (c) profiles of the temperatures of ions and electrons.

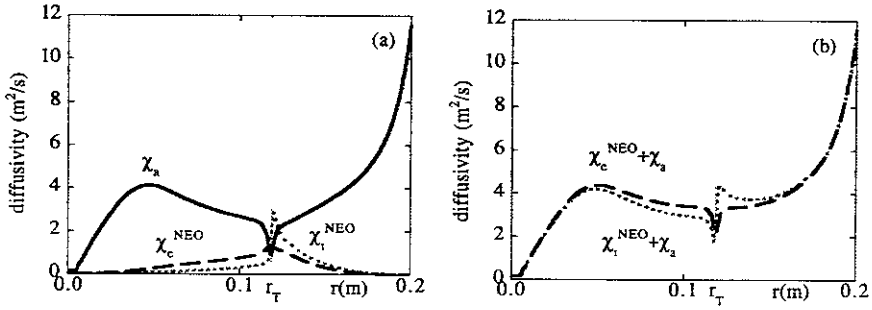

Fig. 2. Radial profiles of the anomalous and neoclassical diffusivities in figure 2(a). In figure 2(b), the sum of the anomalous and neoclassical diffusivities is shown.

solutions exist for the local ambipolar condition. In the case of figure 1(a), the electron root for $r < r_T$ is sharply connected to the ion root for $r > r_T$ with a thin layer between them. The transition point should be determined by the Maxwell construction [13]. We confirm that the Maxwell construction is satisfied in the case of figure 1(a). The profile of the derivative of the radial electric field is observed in figure 1(d). The peak at the transition point $r = r_T$ is found in figure 1(d).

The transport barrier is obtained for the both channels of the neoclassical transport and the anomalous transport, although it is not very clear in both the electron and ion temperature profiles in figure 1(c). In figure 2(a), the anomalous transport diffusivity χ_a is shown with the solid line. At the transition point, the reduction is obtained due to the strong electric field shear. The neoclassical diffusivities of electrons χ_e^{NEO} and ions χ_i^{NEO} are also shown with the dashed line and the dotted line, respectively. In the case of the spatial transition, the electric field goes across zero. Therefore, the neoclassical diffusivities have a peak near the surface where the relation $E_r \approx 0$, because they depend on the value of E_r itself. In figure 2(b), the sum of the anomalous and the neoclassical diffusivities is shown. The case of electrons and the case of ions are obtained with dashed line and the dotted line, respectively. The total suppression can be seen but is small compared with that of the anomalous diffusivity. This is because the neoclassical transport diffusivity has a peak near the radius $r = r_T$.

5 Study of electric field structure in detail

In this section, we investigate the detail of the structure of the electric field shear in the case of the hard transition discussed in the previous section. When the self-consistent analysis by use of the theoretical model for the anomalous transport coefficient is done, the interesting physical issues are obtained

In figure 1(d), there is the difference between the half widths at the half maximum of the inner side ($r < r_T$) and the outer side ($r > r_T$) in the profile of

the electric field shear. The origin of this asymmetry is discussed in ref. [14]. The quantity related with the area $r > r_T$ between the lines of $E_r' = 0$ and E_r' profile is given as

$$\left|\frac{\partial E_r}{\partial r}\right|^2_{right} \approx \frac{1}{\epsilon_0 \epsilon_\perp D_{Ea}} \int_{E_1}^{E_{u1}} J dE_r, \tag{10}$$

where $J = e(\Gamma_i^{na} - \Gamma_e^{na})$, E_1 is the electric field which is the ion root of the local ambipolar condition and E_{u1} is in the range of $E_1 < E_{u1} < E_2$. Here, E_2 is the value of E_r at $r = r_T$. The quantity related with the area $r < r_T$ is shown as

$$\left|\frac{\partial E_r}{\partial r}\right|^2_{left} \approx -\frac{1}{\epsilon_0 \epsilon_\perp D_{Ea}} \int_{E_{u2}}^{E_3} J dE_r, \tag{11}$$

where E_3 is the electric field which is the electron root of the local ambipolar condition and E_{u2} is in the range $E_2 < E_{u2} < E_3$. The quantity $|\partial E_r/\partial r|^2_{right}$ (derived from the ion dominant current) is smaller than that of $|\partial E_r/\partial r|^2_{left}$ (derived from the electron dominant current). Therefore, the asymmetry is obtained and the half width of the inner side is wider than that of the outer side due to the dependence the neoclassical current on the radial electric field.

Next, we compare the solution with the turbulent transport model and that with the constant D_{Ea}. In the case of the constant D_{Ea} [7], the spatial transition occurs to the negative ambipolar solutions before the positive ambipolar solutions of E_r vanishes when the radial point moves outward (shown in figure 3) and the Maxwell's construction holds at the transition point. However, the transition takes place after the positive ambipolar solutions of E_r vanishes in figure 1(a). This is because the there is the contribution from the diffusion term of the electric field (the second term in the right hand side in equation (9)). The condition for the

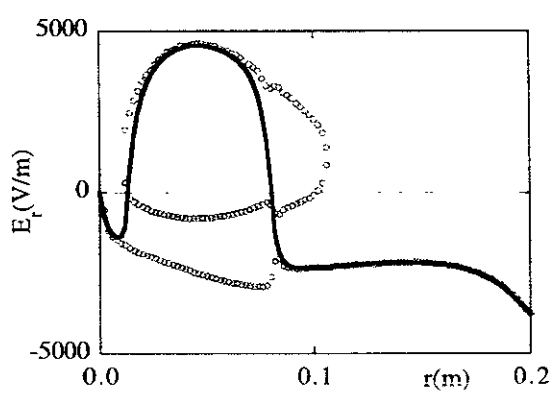

Fig. 3. Profile of the radial electric field in the case of the constant D_{Ea} (solid line). Circles show the solutions which satisfies the local ambipolar condition.

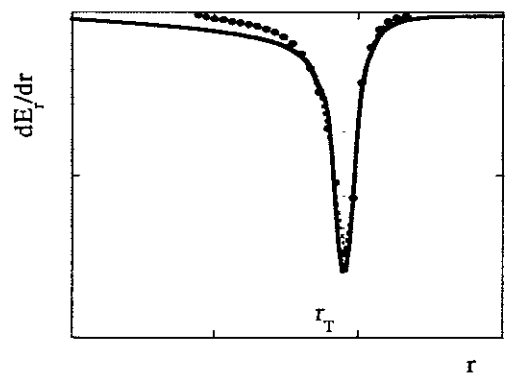

Fig. 4. Schematic figure of the profile of E_r' in the cases of the theoretical model of D_{Ea} (solid line) and the constant D_{Ea} (dashed line).

suppression due to the electric field shear is satisfied where the width in the profile of the electric field shear is smaller than $0.007(m)$.

In figure 4, the spatial profiles of the gradient of E_r are shown in the cases of the anomalous diffusivity D_{Ea} (explained in Sec. 3) as well as of the constant D_{Ea} (shown in figure 3). The anomalous diffusivity D_{Ea} which is reduced due to E_r' is denoted by $D_{Ea}(E_r')$ and the constant D_{Ea} is denoted by $D_{Ea}(const.)$. The solid line represents the case of $D_{Ea}(E_r')$ and the dashed line shows the case of $D_{Ea}(const.)$, respectively. The values of the axes are in the arbitrary units. The value of E_r' is adjusted to be the same width at the half maximum in both cases. It has been known that the peak of $|E_r'|$ and the inverse of the half width depends on $D_{Ea}^{-1/2}$ when D_{Ea} is constant [7]. In order to identify the impact of the trasport reduction, two profiles (results of figure 1(d) and the stretched profile for the case of the constant D_{Ea}) are overlayed in figure 4. The magnitude of the peak of the electric field shear in this study is about twice as that of the case of the constant D_{Ea} which gives the same half width at the half maximum. In the case of the self-consistent solution, the value of $|E_r'|$ is larger away from the interface, therefore, $|E_r'|$ has much prominent tail.

6 Summary and Discussions

In this paper, the structure of the radial electric field in helical plasmas is theoretically studied. The temporal and spatial evolutions of the plasma density, the temperatures and the radial electric field are examined. A numerical formula is employed to determine the neoclassical components of particle and heat fluxes in helical plasmas The analysis is done by use of one-dimensional transport model equations. Theoretical model of the ballooning mode or the interchange mode is adopted for the anomalous heat conductivity and the anomalous diffusion coefficient

of the electric field.

The stationary structure of the radial electric field is shown and the hard transition with the multiple ambipolar E_r is obtained in this study of $T_e/T_i \approx 2$. The connection from the positive electric field (electron root) to the negative electric field (ion root) is seen with the rapid change. The magnitude and the spatial distribution of the transport reduction is examined due to the strong electric field shear. In the case of the electric field interface between the positive E_r and the negative E_r regions, the neoclassical transport takes a peak near the interface. When the value of T_e is much higher than the value of T_i ($T_e/T_i \approx 10$) and the transition type becomes soft (without multiple ambipolar E_r), the gradient of the electric field gets weaker at the electric domain. In that case, no suppression of the anomalous transport diffusivities is obtained and the transport barrier is not seen. The condition for the suppression of the anomalous diffusivities is suggested to be rather high T_i in addition to the low density and high T_e. Compared with the previous analysis of the constant D_{Ea}, the detailed study of the profile of the electric field shear is also done. The difference between the cases of the constant D_{Ea} and this study in the $|E_r'|$ profile near the interface is found. The longer tail in the $|E_r'|$ profile is shown in this study compared to the previous analysis by use of the constant D_{Ea}.

In CHS device, The spatial transition from the larger positive E_r to the smaller positive E_r is observed [2]. Such a spatial transition dose not induce a local peak of χ_j^{NEO}, and should be searched for in simulations. The analysis of the dynamics of the electric field is needed to examine the electric pulsation observed in CHS device[15]. These are left for future studies.

Acknowledgements. The authors would like to acknowledge Prof. S. -I. Itoh, Prof. A. Fukuyama and Dr. M. Yagi for the illuminating discussions. In particular, one of authors (ST) thanks Prof. A. Fukuyama for helpful suggestions relating to the numerical methods. Discussions with Dr. A. Fujisawa, Dr. K. Ida, Dr. H. Sanuki and Dr. H. Sugama are also appreciated. This work is partly supported by a Grant-in-Aid for Scientific Research from the Ministry of Education, Culture, Sports, Science and Technology of Japan.

References

[1] K. Itoh et al : Plasma Phys. Control. Fusion **34** (1994) 123.

[2] A. Fujisawa et al: Phys. Plasmas **7** (2000) 4152.

[3] H. Maassberg et al.: Plasma Phys. Control. Fusion **35** (1993) B319.

[4] M. Kick et al.: Plasma Phys. Control. Fusion **41** (1999) A549.

[5] H. Maassberg et al.: Phys. Plasmas **7** (2000) 295

[6] L. M. Kovriznykh: Nucl. Fusion **24** (1984) 851.

[7] S. Toda and K. Itoh: Plasma Phys. Control. Fusion **43** (2001) 629.

[8] K. Ida: Plasma Phys. Control. Fusion **40** (1998) 1429.

[9] K. C. Shaing: Phys. Fluids **27** (1984) 1567.

[10] D. E. Hastings: Phys. Fluids **28** (1985) 334.

[11] K. Itoh et al.: Plasma Phys. Control. Fusion **36** (1994) 279.

[12] K. Itoh et al.: J. Phys. Soc. Jpn. **62** (1993) 4269.

[13] K. Itoh, S. -I. Itoh and A. Fukuyama: Transport and Structural Formation in Plasmas (London, UK: Institute of Physics Publishing) ch 12.

[14] K. Itoh et al.: J. Plasma Fusion Res. submitted.

[15] A. Fujisawa et al: Phy. Rev. Lett. **81** (1998) 2256.

Recent Issues of NIFS Series

NIFS-678 M Tanaka and A Yu Grosberg,
Giant Charge Inversion of a Macroion Due to Multivalent Counterions and Monovalent Coions Molecular Dynamics Study Jan 2001

NIFS-679 K Akaishi, M Nakasuga, H Suzuki, M Iima, N Suzuki, A Komori, O Motojima and Vacuum Engineering Group
Simulation by a Diffusion Model for the Variation of Hydrogen Pressure with Time between Hydrogen Discharge Shots in LHD Feb 2001

NIFS-680 A Yoshizawa, N Yokoi, S Nisizima, S-I Itoh and K Itoh
Variational Approach to a Turbulent Swirling Pipe Flow with the Aid of Helicity Feb 2001

NIFS-681 Alexander A Shishkin
Estafette of Drift Resonances, Stochasticity and Control of Particle Motion in a Toroidal Magnetic Trap Feb 2001

NIFS-682 H Momota and G H Miley,
Virtual Cathode in a Spherical Inertial Electrostatic Confinement Device Feb 2001

NIFS-683 K Saito, R Kumazawa, T Mutoh, T Seki, T Watari, Y Torii, D A Hartmann, Y Zhao, A Fukuyama, F Shimpo, G Nomura, M Yokota, M Sasao, M Isobe, M Osakabe, T Ozaki, K Narihara, Y Nagayama, S Inagaki, K Itoh, S Morita, A V Krasilnikov, K Ohkubo, M Sato, S Kubo, T Shimozuma, H Idei, Y Yoshimura, O Kaneko, Y Takeiri, Y Oka, K Tsumori, K Ikeda, A Komori, H Yamada, H Funaba, K Y Watanabe, S Sakakibara, M Shoji, R Sakamoto, J Miyazawa, K Tanaka, B J Peterson, N Ashikawa, S Murakami, T Minami, S Ohakachi, S Yamamoto, S Kado, H Sasao, H. Suzuki, K Kawahata, P deVries, M Emoto, H Nakanishi, T Kobuchi, N Inoue, N Ohyabu, Y Nakamura, S Masuzaki, S Muto, K Sato, T Morisaki, M Yokoyama, T Watanabe, M Goto, I Yamada, K Ida, T Tokuzawa, , N Noda, S Yamaguchi, K Akaishi, A Sagara, K Toi, K Nishimura, K. Yamazaki, S. Sudo, Y Hamada, O Motojima, M Fujiwara,
Ion and Electron Heating in ICRF Heating Experiments on LHD Mar 2001

NIFS-684 S Kida and S Goto,
Line Statistics:Stretching Rate of Passive Lines in Turbulence· Mar. 2001

NIFS-685 R Tanaka, T. Nakamura and T Yabe,
Exactly Conservative Semi-Lagrangian Scheme (CIP-CSL) in One-Dimension Mar 2001

NIFS-686 S Toda and K Itoh,
Analysis of Structure and Transition of Radial Electric Field in Helical Systems Mar 2001

NIFS-687 T Kuroda and H Sugama,
Effects of Multiple-Helicity Fields on Ion Temperature Gradient Modes Apr 2001

NIFS-688 M Tanaka,
The Origins of Elctrical Resistivity in Magnetic Reconnection· Studies by 2D and 3D Macro Particle Simulations Apr. 2001

NIFS-689 A Maluckov, N. Nakajima, M Okamoto, S Murakami and R Kanno,
Statistical Properties of the Neoclassical Radial Diffusion in a Tokamak Equilibrium Apr 2001

NIFS-690 Y. Matsumoto, T Nagaura, Y Itoh, S-I Oikawa and T Watanabe,
LHD Type Proton-Boron Reactor and the Control of its Peripheral Potential Structure Apr 2001

NIFS-691 A Yoshizawa, S -I Itoh, K. Itoh and N Yokoi,
Turbulence Theories and Modelling of Fluids and Plasmas Apr 2001

NIFS-692 K Ichiguchi, T Nishimura, N Nakajima, M Okamoto, S -i Oikawa, M Itagaki,
Effects of Net Toroidal Current Profile on Mercier Criterion in Heliotron Plasma Apr 2001

NIFS-693 W Pei, R Horiuchi and T Sato,
Long Time Scale Evolution of Collisionless Driven Reconnection in a Two-Dimensional Open System Apr 2001

NIFS-694 L N Vyacheslavov, K Tanaka, K Kawahata,
CO2 Laser Diagnostics for Measurements of the Plasma Density Profile and Plasma Density Fluctuations on LHD Apr 2001

NIFS-695 T Ohkawa,
Spin Dependent Transport in Magnetically Confined Plasma May 2001

NIFS-696 M Yokoyama, K Ida, H Sanuki, K Itoh, K Narihara, K Tanaka, K Kawahata, N Ohyabu and LHD experimental group
Analysis of Radial Electric Field in LHD towards Improved Confinement May 2001

NIFS-697 M. Yokoyama, K Itoh, S Okamura, K Matsuoka, S -I Itoh,
Maximum-J Capability in a Quasi-Axisymmetric Stellarator May 2001

NIFS-698 S-I Itoh and K. Itoh,
Transition in Multiple-scale-lengths Turbulence in Plasmas: May 2001

NIFS-699 K Ohi, H Naitou, Y Tauchi, O Fukumasa,
Bifurcation in Asymmetric Plasma Divided by a Magnetic Filter May 2001

NIFS-700 H Miura, T Hayashi and T Sato,
Nonlinear Simulation of Resistive Ballooning Modes in Large Helical Device June 2001

NIFS-701 G Kawahara and S Kida,
A Periodic Motion Embedded in Plane Couette Turbulence June 2001

NIFS-702 K. Ohkubo,
Hybrid Modes in a Square Corrugated Waveguide. June 2001

NIFS-703 S.-I Itoh and K Itoh,
Statistical Theory and Transition in Multiple-scale-lengths Turbulence in Plasmas June 2001

NIFS-704 S Toda and K Itoh,
Theoretical Study of Structure of Electric Field in Helical Toroidal Plasmas June 2001